Supporting Information

Engineering a terephthalate-responsive PobR biosensor for discovering PET-degrading microbes via cell-to-cell communication

Jung-Ung An[1,2†], Seok Jin Oh[1,3†], Bong Hyun Sung[1,3,4,5], Seung-Goo Lee[3,4,5], Kil Koang Kwon[1,3,4*], and Dae-Hee Lee[1,3,4,5,6*]

[1]Synthetic Biology Research Center and Korea Biofoundry, Korea Research Institute of Bioscience and Biotechnology (KRIBB), Daejeon 34141, Republic of Korea

[2]Fermentation Convergence Research Group, Korea Food Research Institute (KFRI), Wanju 55365, Republic of Korea

[3]Department of Biosystems and Bioengineering, KRIBB School of Biotechnology, University of Science and Technology (UST), Daejeon 34113, Republic of Korea

[4]Korea Biofoundry, Korea Research Institute of Bioscience and Biotechnology (KRIBB), Daejeon 34141, Republic of Korea

[5]Graduate School of Engineering Biology, Korea Advanced Institute of Science and Technology (KAIST), Daejeon 34141, Republic of Korea

[6]Department of Integrative Biotechnology, College of Biotechnology and Bioengineering, Sungkyunkwan University, Suwon 16419, Republic of Korea

[†]These authors contributed equally to this work.

[*]Correspondence: kkkwon@kribb.re.kr; dhlee@kribb.re.kr

This file includes:

Table S1. Primers used in this study.

Figure S1. Dose-response analysis of PobR_2 toward 4-HB and TPA over the 0-0.5 mM range.

Figure S2. Flow-cytometry analysis of 1,000 single clones recovered after FACS enrichment under 1 mM TPA induction.

Figure S3. Secondary screening of recovered PobR variants in the absence and presence of 1 mM TPA.

Figure S4. Proposed important residues of PobR variant structure.

Figure S5. Sequence logo analysis of amino acid distributions at mutagenized PobR positions recovered during TPA-responsive evolution.

Figure S6. Dose-response comparison of PobR_2 and PobR_3 toward 4-HB and TPA over the 0-1.0 mM range.

Figure S7. Growth curves and fluorescence outputs of PobR_4 in different media.

Figure S8. Growth curves and fluorescence outputs of PobR_4 in 1/10-diluted LB medium.

Figure S9. Colony formation and fluorescence of PobR_4 on solid LB agar containing increasing TPA concentrations.

Figure S10. Colony PCR analysis of colonies recovered from the proof-of-concept screening assay.

Figure S11. Structural comparison of the ligand-binding pockets of wild-type PobR and PobR_v10 with docked TPA.

Table S1. Primers used in this study.

Primer	Sequence (5'-3')
Vector1_F	GAATTCAATGGCGATGACGCATCCTCACGATAAT
Vector1_R	ATGAGCAAAGGTGAAGAACTGTTTACCGGCGTTG
PobR_F	TCATCGCCATTGAATTCTTATACCAAATTACGCA
PobR_R	TCTTCACCTTTGCTCATAACATCATCCTTGCTAT
Vector2_F	AGGACTGAGCTAGCCGTAAAGCGGCCGCGAATTCTTATAC
Vector2_R	TGTTATCCGCTTTAATTAAAAATGGCGATGACGCATCCTC
mMucK_F	GAGGATGCGTCATCGCCATTTTTAATTAAAGCGGATAACA
mMucK_R	GTATAAGAATTCGCGGCCGCTTTACGGCTAGCTCAGTCCT
Vector3_F	AAATTAAAGAGGAGAAAATGAGCAAAGGTGAAGA
Vector3_R	CATATGTATATCTCCTTAACATCATCCTTGCTAT
RacE_F	ATAGCAAGGATGATGTTAAGGAGATATACATATG
RacE_R	TCTTCACCTTTGCTCATTTTCTCCTCTTTAATTT

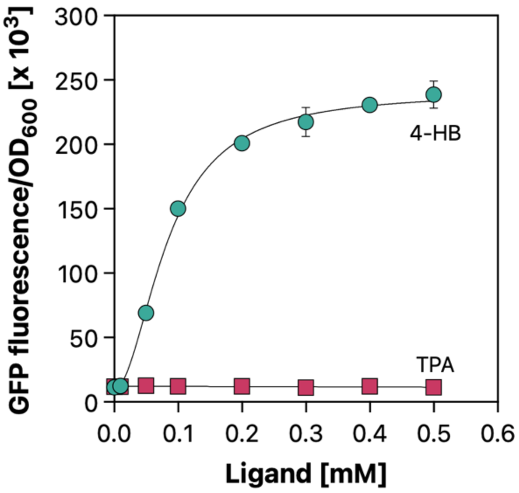

Figure S1. Dose-response analysis of PobR_2 toward 4-HB and TPA over the 0-0.5 mM range. The green circles were indicated fluorescence intensity of PobR_1 cell for 4-HB, the red squares were indicated fluorescence intensity of PobR_1 cell for TPA. The error bars represent the standard deviation.

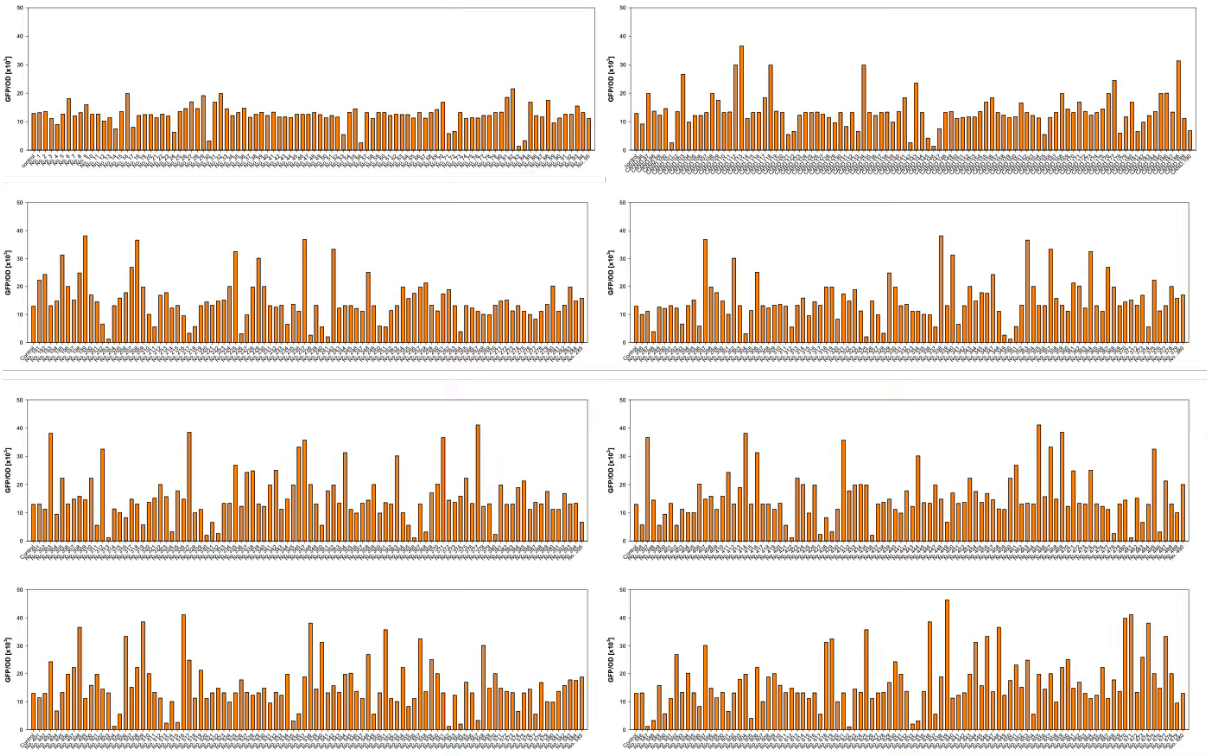

Figure S2. Fluorescence screening of 1,000 single clones recovered after FACS enrichment under 1 mM TPA induction. Recovered clones were individually cultured and analyzed for GFP output to identify variants with increased TPA-responsive fluorescence.

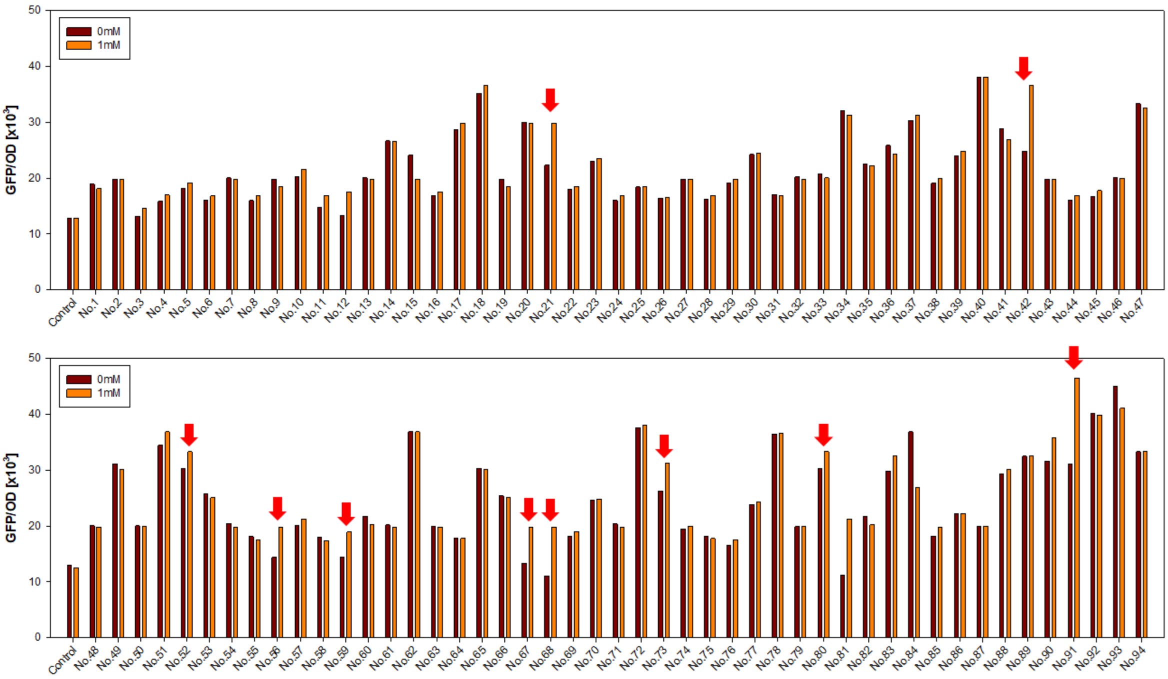

Figure S3. Secondary screening of recovered PobR variants in the absence and presence of 1 mM TPA. Recovered variants were cultured with or without 1 mM TPA, and GFP fluorescence normalized by cell density was measured to identify TPA-responsive clones. Arrows indicate selected variants showing increased TPA-dependent activation.

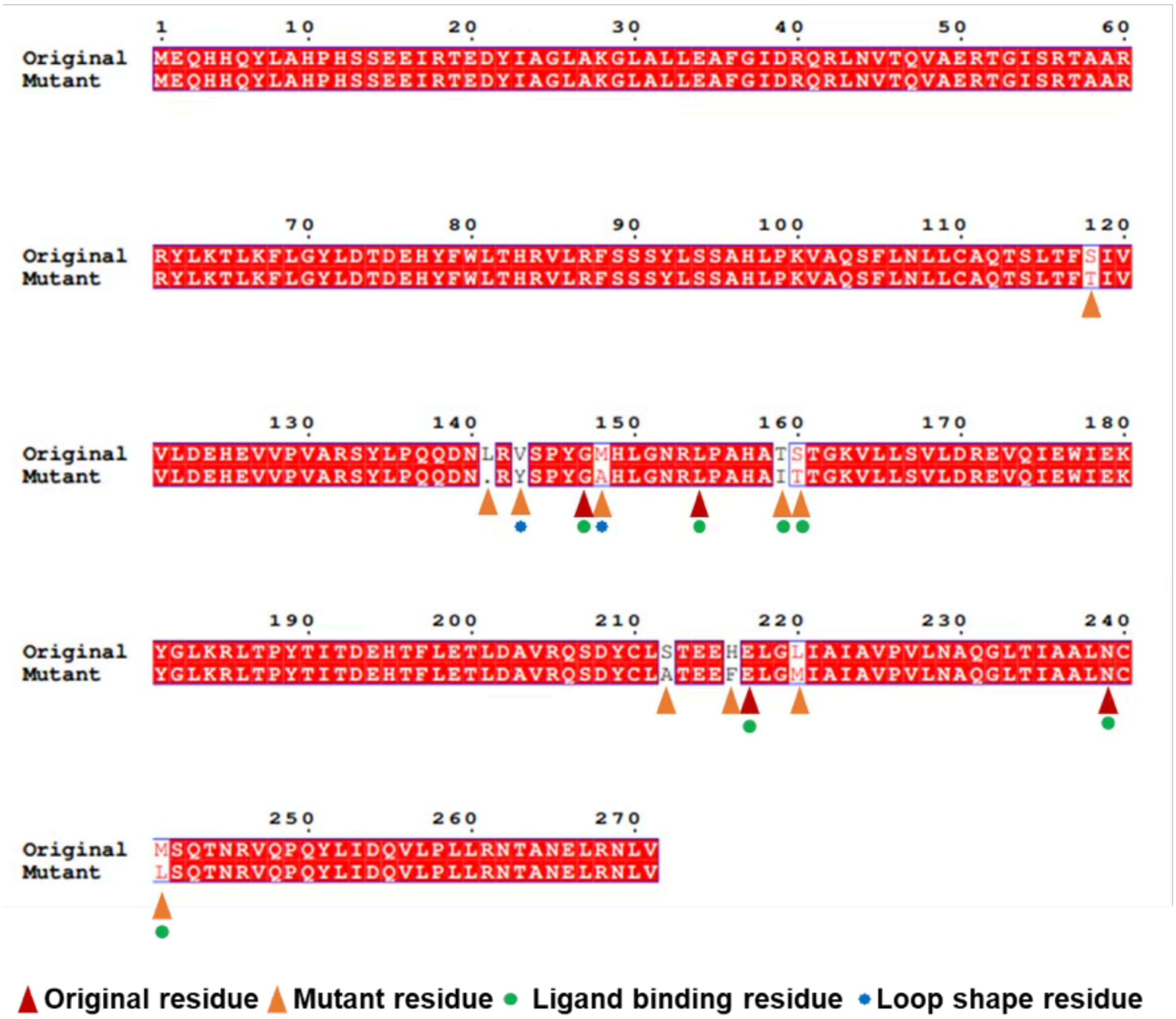

Figure S4. Sequence comparison of wild-type PobR and the evolved PobR_v10 variant. Amino acid sequences of wild-type PobR and PobR_v10 are aligned, with mutated residues indicated by triangles. Wild-type and substituted residues are highlighted in red and yellow, respectively. Residues predicted to be located near the modeled TPA-binding region are marked with green circles, whereas residues associated with loop remodeling are indicated by blue circles.

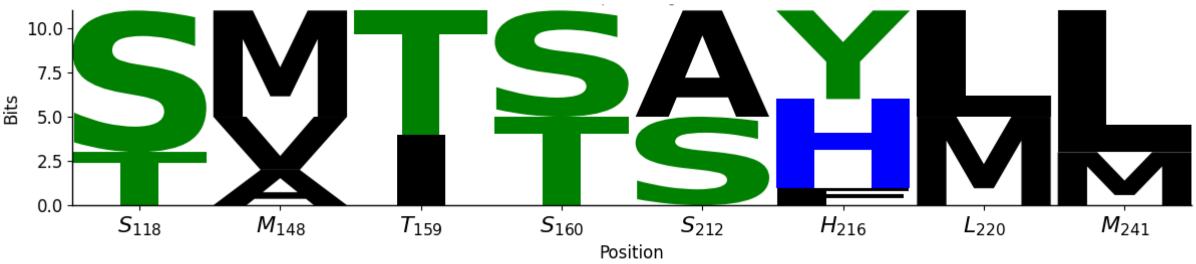

Fig S5. Sequence logo analysis of amino acid distributions at mutagenized PobR positions recovered during TPA-responsive evolution. Sequence logo representation of amino acid distributions at the eight displayed mutagenized positions (S118, M148, T159, S160, S212, H216, L220, and M241) identified across PobR variants (v1–v10) during directed evolution toward TPA responsiveness. Letter height is proportional to the frequency of each amino acid at the corresponding position among the recovered variants

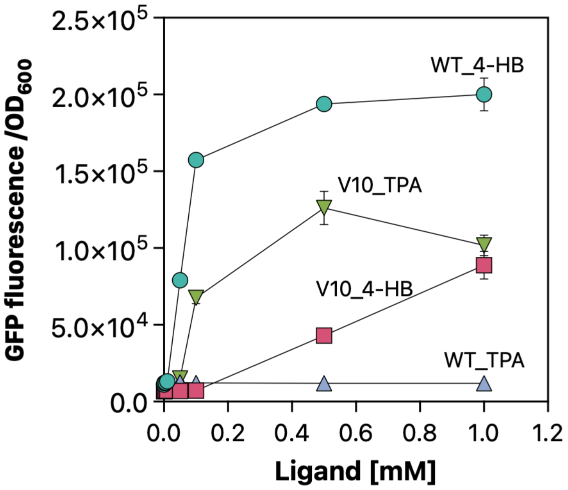

Figure S6. Dose-response comparison of PobR_2 and PobR_3 toward 4-HB and TPA over the 0-1.0 mM range. Green circles indicate the fluorescence intensity of PobR_2 in response to 4-HB, and yellow circles indicate the fluorescence intensity of PobR_2 in response to TPA. Blue circles indicate the fluorescence intensity of PobR_3 in response to 4-HB, whereas pink circles indicate the fluorescence intensity of PobR_3 in response to TPA. Error bars represent the standard deviation of duplicate experiments.

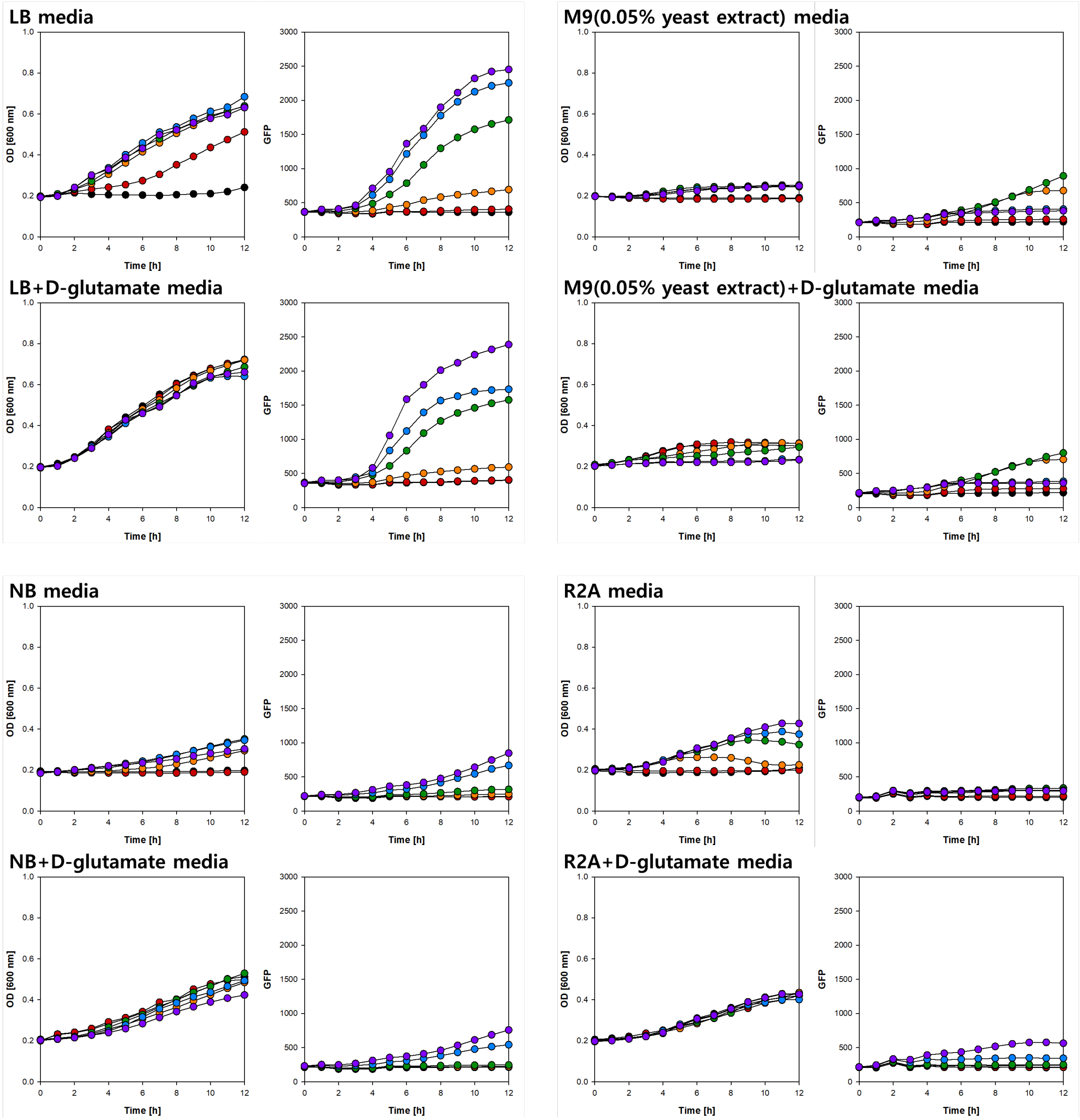

Figure S7. Growth curves and fluorescence outputs of PobR_4 in different media. PobR_4 cells were grown in LB, NB, M9, and R2A media with or without D-glutamate. Black, red, yellow, green, blue, and purple circles indicate TPA concentrations of 0, 0.01, 0.05, 0.1, 0.5, and 1 mM, respectively.

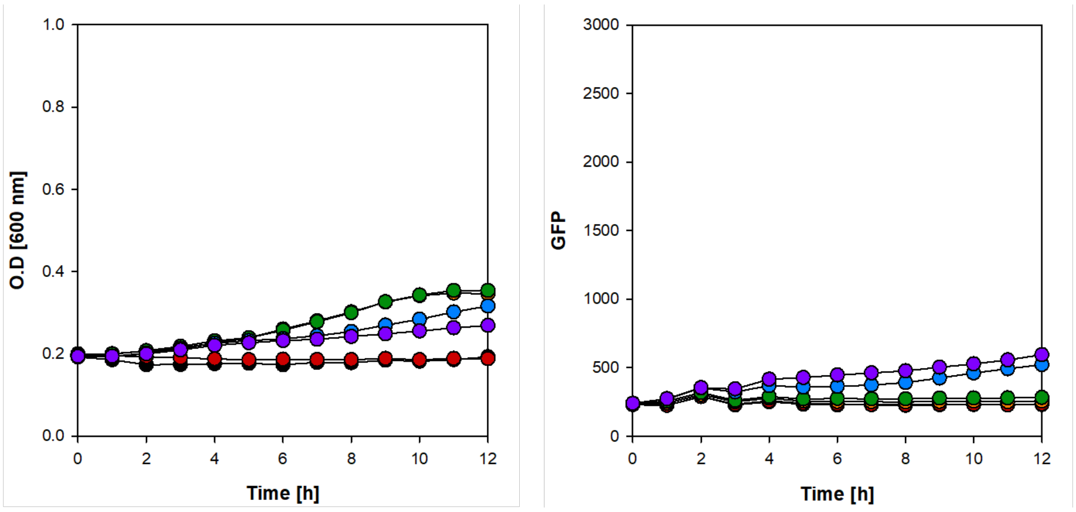

Figure S8. Growth curves and fluorescence outputs of PobR_4 in 1/10-diluted LB medium. PobR_4 cells were grown in 1/10-diluted LB medium with or without D-glutamate. Black, red, yellow, green, blue, and purple circles indicate TPA concentrations of 0, 0.01, 0.05, 0.1, 0.5, and 1 mM, respectively.

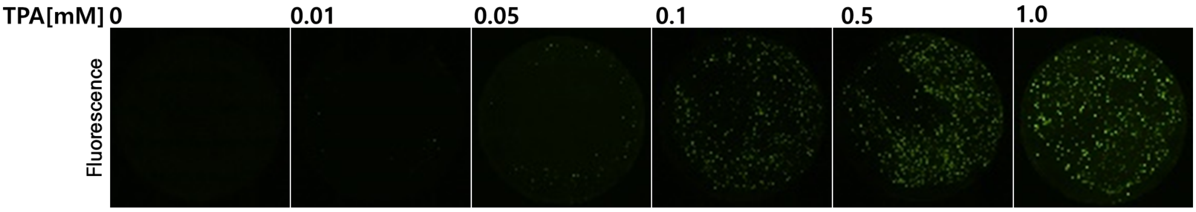

Figure S9. Colony formation and fluorescence of PobR_4 on solid LB agar containing increasing TPA concentrations. PobR_4 cells were plated on LB agar without D-glutamate and supplemented with the indicated concentrations of TPA. Colony formation and fluorescence increased in a TPA concentration-dependent manner.

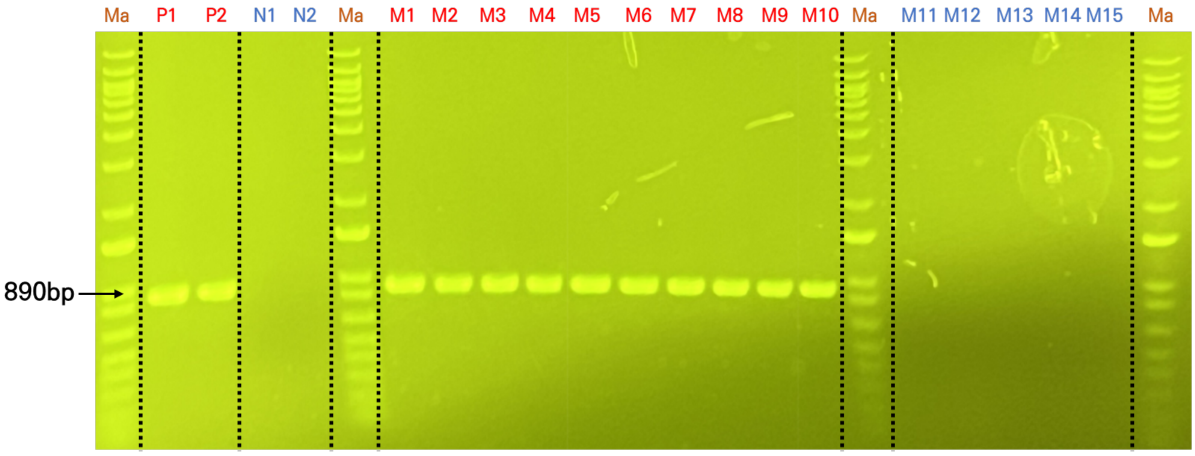

Figure S10. Colony PCR analysis of colonies recovered from the proof-of-concept screening assay. P1 and P2 were selected from positive-control plates, N1 and N2 were selected from negative-control plates, and M1–M15 were selected from mixed plates. The expected 890-bp lcc amplicon was detected in colonies associated with surrounding biosensor fluorescence, confirming the presence of the LCC expression construct.

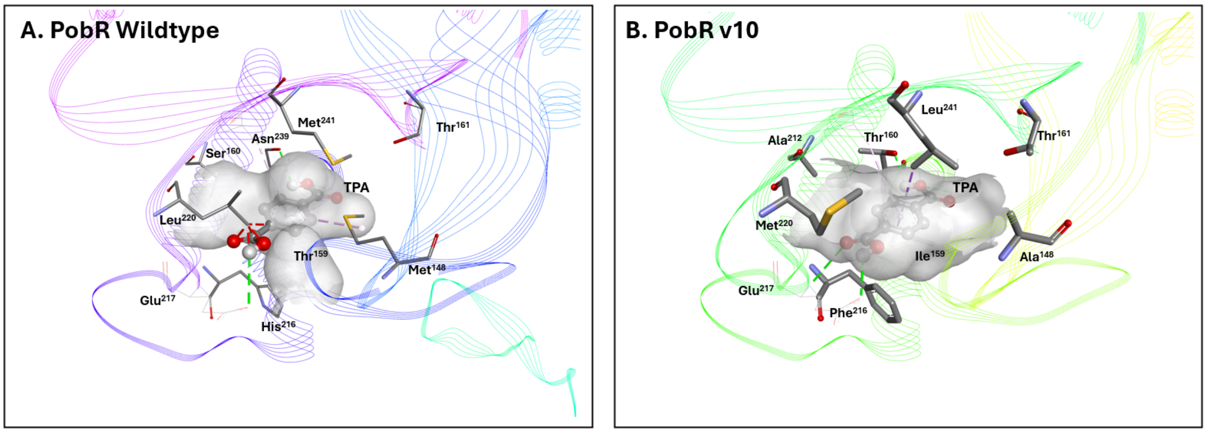

Figure S11. Structural comparison of the predicted ligand-binding pockets of wild-type PobR and PobR_10 with docked TPA. (A) Predicted ligand-binding pocket of wild-type PobR with TPA mapped onto the model. In the wild-type configuration, Met148 and Leu220 are predicted to create steric constraints near the pocket interior, potentially limiting productive accommodation of TPA. Red dashed lines indicate predicted steric constraints. Glu217 is positioned away from the distal carboxylate group of TPA in this configuration. (B) Predicted ligand-binding pocket of PobR_10 with docked TPA. The surface representation suggests an expanded local pocket geometry relative to wild-type PobR, which may help accommodate the distal carboxylate group of TPA. Predicted interactions and pocket changes should be interpreted as computational hypotheses rather than experimentally resolved structural features.